Implications for High Frequency Gravitational Wave from the PTA Data

Junsong Cang[1],* Yu Gao[2],† Yi-ming Liu[3],‡ and Sichun Sun[3]§
[1] *School of Physics, Henan Normal University, Xinxiang, China*
[2] *Key Laboratory of Particle Astrophysics, Institute of High Energy Physics, Chinese Academy of Sciences, Beijing 100049, China and School of Physics, Beijing Institute of Technology, Beijing, 100081, China*

Recently several pulsar timing array (PTA) experiments such as NANOGrav and PPTA reported detection of a gravitational wave (GW) background at nano-Hz frequency band. Enhanced curvature perturbation $P_{\mathcal{R}}$ can produce scalar induced gravitational wave (SIGW) that serves as a good source candidate for the observed GW signal. Here we show that if the PTA signal were indeed of SIGW origin, $P_{\mathcal{R}}$ amplitude required will produce primordial black holes (PBHs) in $[2\times10^{-5}, 2\times10^{-2}]\ m_\odot$ mass range. Mergers of these PBHs will produce strong gravitational wave (GW) background in $[10^{-3}, 10^{8}]$ Hz frequencies that falls into the sensitivity reach of various high frequency GW observatories such as the Einstein Telescope (ET), DECIGO and BBO, which can help further scrutinize the SIGW interpretation of PTA signal.

Introduction Enthusiasm in primordial black holes (PBHs) [1, 2] has grown immensely after the LIGO discovery of gravitational wave signals [3] in agreement with merger events of black holes above stellar masses [4]. With sufficiently large primordial curvature perturbation $\mathcal{R}$, such black holes can be produced in the early Universe from gravitational collapse of overdense regions. PBHs are under extensive searches for their astrophysical signals, see Ref. [5] for a recent review. The early process of over-density collapse is also predicted to release scalar-induced gravitational waves (SIGW) [6, 7], which offers a glimpse at valuable information of early fluctuations at late-time gravitational wave detectors.

The primordial black hole can be supermassive, to generate gravitational waves from the mergers directly. In the case of the scalar-induced gravitational waves(SIGW), the associated PBH produced in this case is a couple of orders below solar mass, and the mergers of such light PBH produced a gravitational wave signal around Mhz. Since the endeavor of the whole gravitational wave frequency spectrum searches has begun, with various proposals already in Mhz-Ghz band[8], it is intriguing to link the ultra-low NanoHz gravitational waves to the ultra-high frequency gravitational searches. We may call it a multi-messager task in the frequency spectrum space.

In recent month, several Pulsar Timing Array (PTA) observatories including NANOgrav [9], Chinese PTA (CPTA) [10], Parkes PTA (PPTA) [11] and European PTA [12, 13] reported strong evidence for gravitational wave (GW) background at nano-Hertz waveband, which verifies previous claims from [14–17]. These observations incited several studies on potential sources of observed GW background [18], such as supermassive black holes [19, 20], phase transition [21–24] and axion topological defects [25–27].

In case of SIGW from overdensity collapse, a GW signal at PTA's nHz frequency generally requires a curvature power spectrum $P_{\mathcal{R}}$ with large amplitude at the scale of $k \sim 10^8$ Mpc^{-1} [18, 19]. At large scales ($k \lesssim 10$Mpc^{-1}), $P_{\mathcal{R}}$ has been well constrained by observations from cosmic mircrowave background (CMB) and large scale structures [28, 29], however at smaller scales $P_{\mathcal{R}}$ is comparably poorly constrained [7] and can potentially has amplitude large enough to explain PTA signal.

In this letter, we show that $P_{\mathcal{R}}$ amplitude required for generating SIGW compatible with PTA data will also lead to formation of PBHs with mass in $[2\times10^{-5}, 2\times10^{-2}]m_\odot$ range. The mergers of these PBHs can produce GW background peaked at around MHz frequencies, which can be easily detected by various high frequency GW observatories such as Einstein Telescope (ET) [30], Deci-Hertz Interferometer Gravitational Wave Observatory (DECIGO) [31] and Big Bang Observer (BBO) [32]. This work is structured as follows, we begin by a review of our model for SIGW and merging PBH. After discussing our inference settings we present our results and conclusions.

GW from curvature perturbation and PBH mergers. As a good approximation for a large class of curvature perturbation models, we consider a log-normal parameterization for curvature power spectrum $P_{\mathcal{R}}$ [18, 19, 33–35],

$$P_{\mathcal{R}} = \frac{A}{\sqrt{2\pi\Delta^2}} \exp\left[-\frac{(\ln k/k_*)^2}{2\Delta^2}\right] \tag{1}$$

where A, k_* and Δ are model parameters, which describe the amplitude, peak location and the width of $P_{\mathcal{R}}$ respectively. Upon horizon crossing, $P_{\mathcal{R}}$ will modify the radiation quadruple moment and generate SIGW at second order. If sufficiently large, $P_{\mathcal{R}}$ will also generate overdense regions that can gravitationally collapse and form PBHs [7]. Here we find that the PBHs generated by $P_{\mathcal{R}}$

*Electronic address: cangjunsong@outlook.com
†Electronic address: gaoyu@ihep.ac.cn
‡Electronic address: 7520220161@bit.edu.cn
§Electronic address: sichunssun@bit.edu.cn

spectrum in Eq. (1) has a mass distribution that can be well fit by a log-normal profile [7],

$$\psi = f_{\rm bh}\frac{1}{\sqrt{2\pi}\sigma_{\rm bh}}\exp\left[-\frac{\ln^2(m/m_{\rm c})}{2\sigma_{\rm bh}^2}\right], \tag{2}$$

where $\psi \equiv {\rm d}f_{\rm bh}/{\rm d}\ln m$, $f_{\rm bh} \equiv \rho_{\rm bh}/\rho_{\rm dm}$ is the fraction of DM made of PBHs, $\rho_{\rm bh}$ and $\rho_{\rm dm}$ denotes mass densities of PBH and DM respectively, m denotes PBH mass, $m_{\rm c}$ and $\sigma_{\rm bh}$ are peak and width of the distribution respectively. For convenience, in what follows we will parameterise our PBH distribution using Eq. (2).

In addition to SIGW, merger events of PBH binaries created by $P_{\mathcal{R}}$ can also emit GW at higher frequencies. The comoving merger rate R of a pair of PBHs with mass m_1 and m_2 is given by [36],

$$\begin{aligned}\frac{{\rm d}R}{{\rm d}m_1{\rm d}m_2} \simeq \frac{1.6\times10^6}{{\rm Gpc^3yr}} f_{\rm bh}^{-\frac{21}{37}}\eta^{-\frac{34}{37}}\left(\frac{M}{m_\odot}\right)^{-\frac{32}{37}} \\ \times\left(\frac{t}{t_0}\right)^{-\frac{34}{37}} S\psi(m_1)\psi(m_2)\end{aligned} \tag{3}$$

where $M = m_1 + m_2$, $\eta = m_1m_2/M^2$, t is the time of merger, $t_0 = 13.8$Gyr is the current age of the Universe. S is a suppression factor which takes the form [36, 37],

$$S = \frac{{\rm e}^{-\bar{N}(y)}}{\Gamma(21/37)}\int {\rm d}v v^{-\frac{16}{37}}\exp\left[-\phi - \frac{3\sigma_{\rm M}^2v^2}{10f_{\rm bh}^2}\right] \tag{4}$$

$$\phi = \frac{\bar{N}(y)\,\langle m\rangle}{f_{\rm bh}}\int\frac{{\rm d}m}{m}\psi(m)F\left(\frac{M}{\langle m\rangle}\frac{v}{\bar{N}(y)}\right) \tag{5}$$

where $\sigma_{\rm M} \simeq 0.004$, $\bar{N}(y)$ is the expected number of PBHs within a comoving radius of y around the binary [38], and we take $\bar{N}(y) \simeq Mf_{\rm bh}/[\langle m\rangle(f_{\rm bh}+\sigma_{\rm M})]$ following [36–38], which has been shown to agree well with numerical simulation for $f_{\rm bh} \leq 0.1$ [36, 38]. $\langle m\rangle$ is the mean of PBH mass over number density distribution [37], which equals $m_{\rm c}{\rm e}^{-\sigma_{\rm bh}^2/2}$ for our log-normal mass distribution in Eq. (2). $F(z) =_1 F_2(-1/2, 3/4, 5/4; -9z^2/16) - 1$, ${}_1F_2$ is the generalized hypergeometric function.

The energy density for merging PBHs is calculated as [39],

$$\Omega_{\rm GW} = \frac{f}{\rho_{\rm cr}}\int\frac{{\rm d}z{\rm d}R}{(1+z)H}\frac{{\rm d}E_{\rm GW}(f_{\rm r})}{{\rm d}f_{\rm r}} \tag{6}$$

here $\Omega_{\rm GW} \equiv \rho_{\rm cr}^{-1}{\rm d}\rho_{\rm GW}/{\rm d}\ln f$ is fractional GW density per log frequency interval, $\rho_{\rm GW}$ and $\rho_{\rm cr}$ are GW density and current critical density respectively, $f_{\rm r} = (1+z)f$ is the source frequency, ${\rm d}E_{\rm GW}(f_{\rm r})/{\rm d}f_{\rm r}$ is the source energy spectrum for each individual PBH merger event, for which we adopt [40], $H = H_0[\Omega_\Lambda + \Omega_{\rm m}(1+z)^3 + \Omega_{\rm r}(1+z)^4]^{1/2}$ denotes Hubble parameter, and we use the Planck 2018 [29] of $H_0 = 67.66$ kms^{-1}Mpc^{-1}, $\Omega_\Lambda = 0.6903$ and $\Omega_{\rm m} = 0.3096$. We assume massless neutrino such that the radiation density fraction $\Omega_{\rm r} = 9.1\times10^{-5}$.

Inference Settings To find the credible region for PBHs and the corresponding merger GW signal, we analyzed the PTA datasets using our SIGW model. Our log-likelihood takes the form,

$$\ln\mathcal{L} = -\frac{1}{2}\sum_i\frac{(x_i-u_i)^2}{\sigma_i^2} \tag{7}$$

here the index i denotes frequency, x is $\Omega_{\rm GW}$ for our SIGW model, u is the measured median for $\Omega_{\rm GW}$, σ is the error bar for $\Omega_{\rm GW}$, which equals σ_u for $x > u$ and σ_l otherwise, where σ_u and σ_l are upper and lower error bars respectively. We used PTA GW datasets from NanoGrav [9], IPTA [17] and PPTA [11] in our inference. For convenience, we follow [18] and estimate the signal median and error bars for each experiment directly using the $\Omega_{\rm GW}$ posterior summarised in [41, 42], and we have checked that our results (when using NG15 data only) agrees very well with that shown in [18] and [19] .

As a form of dark radiation, the extra energy budget from SIGW will also change the effective degree of relativistic degrees of freedom $N_{\rm eff}$. In Planck 2018 results (hereafter PLK) [29], a joint analysis of datasets from CMB, baryon acoustic oscillations (BAO) and Big Bang Nucleosynthesi (BBN) constrain $N_{\rm eff}$ to [7, 29],

$$\Delta N_{\rm eff} \equiv N_{\rm eff} - 3.046 \leq 0.175,\ 95\%\ {\rm C.L.} \tag{8}$$

this translates into an upper bound on integrated GW density of $\int{\rm d}\ln f\Omega_{\rm GW} < 2.1\times10^{-6}$ [7], here 3.046 is the value of $N_{\rm eff}$ predicted by the standard model of particle physics [7, 29, 43]. To accomodate the PLK $N_{\rm eff}$ limits, we added a prior of $\Delta N_{\rm eff} < 0.175$ to our inference. Since $f_{\rm bh}$ in our mass range has been constrained to $\mathcal{O}(0.1)$ [44], we also use a prior of $f_{\rm bh} \in [10^{-20}, 10^{-1}]$, this ensures that PBH does not violate the existing abundance constraints while still has physically meaningful abundance for appreciable merger GW production. For completeness, we consider a total of 3 inference settings:

- **GW**: Use PTA GW data alone.
- **GW + $\Delta N_{\rm eff}$**: Use PTA GW data and PLK $\Delta N_{\rm eff}$ limits in Eq. (8).
- **GW + $\Delta N_{\rm eff}$ + PBH**: Use PTA GW data and PLK $\Delta N_{\rm eff}$ limits along with the prior of $f_{\rm bh} \in [10^{-20}, 10^{-1}]$.

Results We sampled the likelihoods in Eq. (7) using the `multinest` sampler [45], and we compute constraints for our $P_{\mathcal{R}}$ parameters and various derived observables (e.g. $\Delta N_{\rm eff}$, PBH parameters and merger GW) by analyzing the `multinest` chains using the `GetDist` package [46]. Tab.I summarises the prior ranges for our parameters along with their marginalised confidence region. Fig. 1 visualises the marginalised posterior from our inference, the left panel shows the results for our $P_{\mathcal{R}}$ model parameters and the derived $\Delta N_{\rm eff}$ from different inference settings, the right panel shows the results for PBH parameters $f_{\rm bh}$, $m_{\rm c}$ and $\sigma_{\rm bh}$.

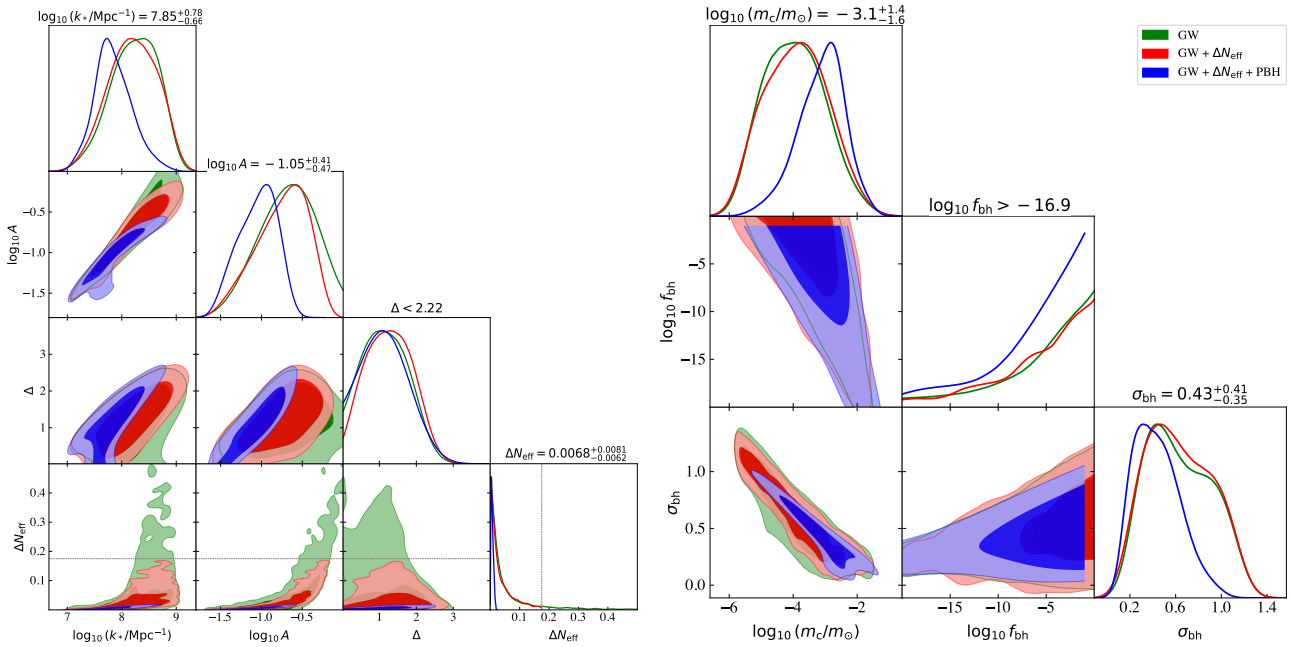

FIG. 1: Marginalised posteriors for our $P_{\mathcal{R}}$ parameters (k_*, A, Δ) and the derived $\Delta N_{\rm eff}$ and PBH parameters $(m_{\rm c}, f_{\rm bh}, \sigma_{\rm bh})$. The green, red and blue contours correspond to GW, GW + $\Delta N_{\rm eff}$, GW + $\Delta N_{\rm eff}$ + PBH inference settings respectively. Light and dark shaded regions correspond to 68% and 95% confidence levels respectively. The dotted line in the $\Delta N_{\rm eff}$ panels indicates the PLK upper limit of $\Delta N_{\rm eff} < 0.175$, numbers on the diagonal panels show the marginalised mean and 95% confidence region from our main GW + $\Delta N_{\rm eff}$ + PBH setting.

Parameters	Prior range	95% Limits GW	95% Limits GW+$\Delta N_{\rm eff}$ + PBH
$\log_{10} A$	[-1.8, 0]	[-1.3, -0.0]	[-1.51, -0.63]
$\log_{10}(k_*/{\rm Mpc}^{-1})$	[6.8, 9.0]	[7.4, 9.0]	[7.2, 8.6]
Δ	[0.02, 4]	[0.02, 2.2]	[0.02, 2.22]
$\log_{10} f_{\rm bh}$	[-20, -1]	[-13.6, 10.2]	[-16.9, -1]
$\log_{10}[m_{\rm c}/m_\odot]$	–	[-5.7, -2.1]	[-4.7, -1.7]
$\sigma_{\rm bh}$	–	[0.15, 1.17]	[0.08, 0.84]
$\Delta N_{\rm eff}$	≤ 0.175	[0, 0.36]	[0.006, 0.014]

TABLE I: Parameters in our inference and their allowed range and marginalised 95% C.L. limits. A, k_* and Δ are our free model parameters, whereas $f_{\rm bh}$, $m_{\rm c}$, $\sigma_{\rm bh}$ and $\Delta N_{\rm eff}$ are parameters derived from A, k_* and Δ. Note that GW data alone overproduces PBHs by about 10 orders of magnitude.

As can be seen from the left panel of Fig. 1 and from Tab.I, using GW data alone gives a marginalised $\Delta N_{\rm eff}$ 95% C.L upper bound of 0.36, which is about 2σ away from the PLK upper limit, and adding the prior in Eq. (8) leads to a tighter constraints. In both these inference settings, the derived posterior for $f_{\rm bh}$ can reach beyond the physically forbidden region of $f_{\rm bh} \geq 1$ by more than 10 orders of magnitude, and after adding the physically motivated $f_{\rm bh} < 0.1$ prior, our constraints tightens significantly. In GW fitting, $m_{\rm c}$ and $\sigma_{\rm bh}$ are constrained (at 95% C.L.) to $[1.8\times10^{-6}, 7.5\times10^{-2}]$ $m_\odot$ and [0.15, 1.17] respectively, and in the GW+$\Delta N_{\rm eff}$+PBH fitting, constraint tightens to $[2\times10^{-5}, 2\times10^{-2}]$ $m_\odot$ for $m_{\rm c}$ and [0.08, 0.84] for $\sigma_{\rm bh}$.

In the green colored regions of Fig. 2, we show the 95 % C.L. posterior for the merger GW (left) and merger rate (right) derived from our main GW+$\Delta N_{\rm eff}$+PBH inference, and the black solid curves correspond to the maximum likelihood best-fit values of $f_{\rm bh} = 0.1$, $m_{\rm c} = 2.6\times10^{-4} m_\odot$ and $\sigma_{\rm bh} = 0.54$. Our $\Omega_{\rm GW}$ posterior peaks at around 10 MHz with an amplitude of $\mathcal{O}(10^{-8})$, which falls into the frequency range of various high frequency GW observatories such as DMRadio and Levitated Sensors [8]. Towards lower frequencies $\Omega_{\rm GW}$ decays as $f^{2/3}$, and below 10^4 Hz, $\Omega_{\rm GW}$ starts to fall into the sensitivity reach of various proposed experiments [6, 47, 48], such as Cosmic Explorer (CE) [49], Einstein Telescope (ET) [30], Deci-Hertz Interferometer Gravitational Wave Observatory (DECIGO) [31] and Big Bang Observer (BBO) [32]. For DECIGO and BBO in particular, $\Omega_{\rm GW}$ posterior strength exceeds the sensitivity reach by about a factor of 10^3 and 10^5, indicating a positive prospect for experimental searches. The right panel of Fig. 2 shows that our inference constrains the merger rate today to $R \lesssim 4\times10^7$ Gpc^{3}yr^{-1}. Since $R \propto t^{-34/37}$ (see Eq. (3)) and that $t \propto (1+z)^{-1.49}$ for $z \in [0, 200]$, our posterior for R scales roughly as $R \propto (1+z)^{1.4}$.

In both panels we also show the result when the $f_{\rm bh} < 0.1$ prior is lifted to $f_{\rm bh} < 1$, which is equivalent to requiring the density of PBH to not exceed that of

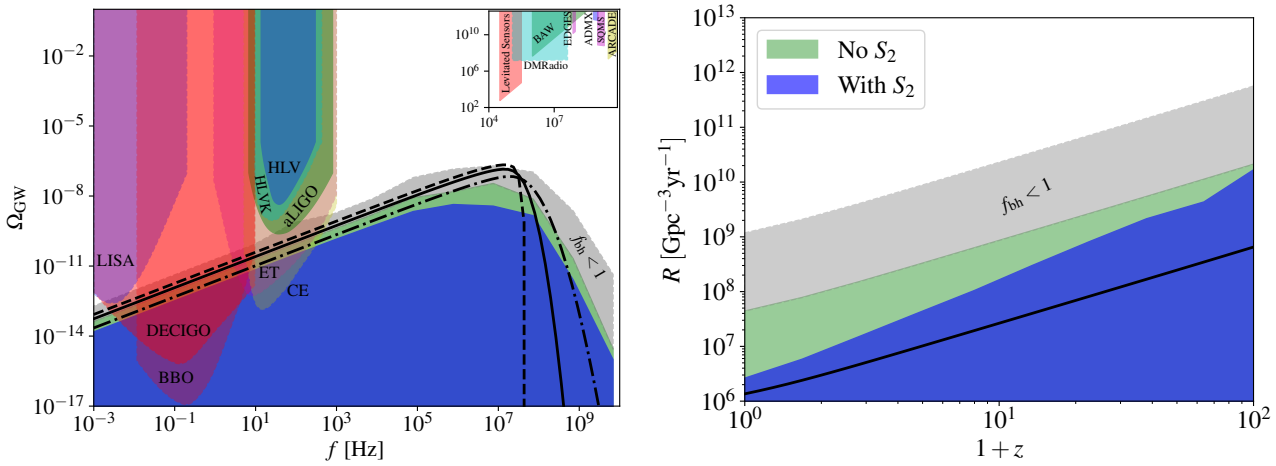

FIG. 2: 95% C.L. confidence region for merger $\Omega_{\rm GW}$ (left) and merger rate (right) from GW + $\Delta N_{\rm eff}$ + PBH inference, legend applies to both panels. The green (blue) regions show the posterior when halo disruption of PBH binary (see Eq. (9)) is ignored (considered). We also show results when $f_{\rm bh} < 0.1$ prior has been lifted to $f_{\rm bh} < 1$ (ignoring the S_2 term in Eq. (9)), however for $f_{\rm bh} > 0.1$ the robustness of our merger calculation is yet to be verified, thus we mark these regimes with grey regions. The solid black lines correspond to our best-fit PBH parameters of $f_{\rm bh} = 10^{-1}$, $m_{\rm c} = 2.6 \times 10^{-4} m_\odot$, $\sigma_{\rm bh} = 0.54$. In the left panel, we also show $\Omega_{\rm GW}$ computed for $\sigma_{\rm bh} = 0$ (monochromatic PBHs, dashed) and $\sigma_{\rm bh} = 1$ (dot-dashed), with the $f_{\rm bh}$ and $m_{\rm c}$ fixed to 0.1 and $2.6 \times 10^{-4} m_\odot$ respectively. We also show the experimental sensitivities of LISA, DECIGO, BBO, ET, CE, aLIGO, Levitated Sensors, BAW, DMRadio, SQMS and ARCADE. Sensitivities below kHz frequencies are the power law integrated sensitivities taken from Refs [6, 47, 48], and sensitivities above kHz are calculated from the strain $h_{\rm c}$ sensitivities collected in [8] via $\Omega_{\rm GW} = 2\pi^2 f^2 h_{\rm c}^2/(3H_0^2)$ [47]. Existing and proposed experiments are indicated by solid and dashed edges respectively. The grey dotted line roughly corresponds to the $\Omega_{\rm GW}$ upper limit indicated by the PLK $\Delta N_{\rm eff}$ limit of $\Delta N_{\rm eff} < 0.175$ (or $\int {\rm d} \ln f \Omega_{\rm GW} < 2.1 \times 10^{-6}$ [7]).

DM. It should be note however that the robustness of the $\bar{N}(y)$ expression we used in Eq. (4) is yet to be tested for $f_{\rm bh} > 0.1$ [36, 38], thus caution should taken when using our result at such regimes and we indicate these regions with grey colors and dashed edges. With this caveat in mind, Fig. 2 shows that $f_{\rm bh} < 1$ prior increases the $\Omega_{\rm GW}$ posterior by about a factor of 5 and into the sensitivity reach of advanced LIGO (aLIGO) [48] and LISA (Laser Interferometer Space Antenna) [50], whereas the posterior for merger rate R is levitated by about a factor of 60.

As structure formation begins, PBH binaries may collide with DM halos containing PBH clusters [37, 51], which disrupts the binary and thereby suppressing the PBH merger rate at lower redshifts. This effect can be accounted for by multiplying the differential merger rate in Eq. (3) by an additional suppression term S_2 [37],

$$S_2 \simeq \min\left[1, 1.96 \times 10^{-3} x^{-0.65} \exp\left(0.03 \ln^2 x\right)\right] \quad (9)$$

here $x = (t/t_0)^{0.44} f_{\rm bh}$. We show results for this scenario in the blue contours of Fig. 2, and it can be seen that this lowers $\Omega_{\rm GW}$ posterior by about a factor of 3, and the corresponding merger rate posterior is reduced to about $R \lesssim 2.6 \times 10^6$ Gpc^{3}yr^{-1}.

Conclusions Enhanced curvature perturbation $P_{\mathcal{R}}$ can produce SIGW which serves as a good source candidate of the GW signal recently reported by various PTA experiments. This letter scrutinizes the implication of this scenario at higher frequency band of GW spectrum. We show that if the PTA GW signal were indeed sourced by SIGW, the $P_{\mathcal{R}}$ amplitude required will create PBHs in $[2 \times 10^{-5}, 2 \times 10^{-2}]$ $m_\odot$ mass range. Mergers of these PBHs will produce strong GW background across $[10^{-3}, 10^8]$ Hz frequencies, which falls into the sensitivity reach of various proposed GW projects such as Einstein Telescope (ET), Cosmic Explorer (CE), DECIGO and BBO, thus the high frequency GW experiments can help verify whether the PTA GW signal is sourced by SIGW.

Acknowledgements. J.C would like to thank Gabriele Franciolini and Paul Frederik Depta for helpful discussions about data analysis and the calculation of merger GW.

Appendix A: Production of SIGW and PBHs from curvature perturbation

Upon horizon crossing, $P_{\mathcal{R}}$ will modify the radiation quadruple moment and generate SIGW at second order, whose energy density per log frequency interval today is given by [7, 33, 52, 53]

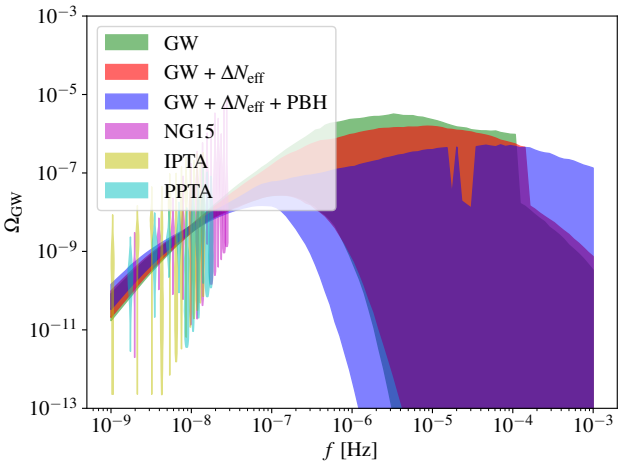

FIG. 3: Posterior distribution of SIGW and a comparison with experimental data.

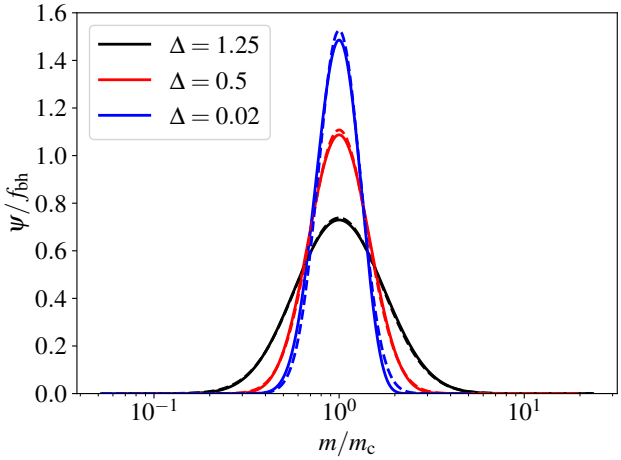

FIG. 4: Accuracy of the fit in Eq. (2). Solid lines show the actual ψ profile computed by Eq. (A5), dashed lines designate the best-fit log-normal profile using Eq. (2). In all curves we take $A = 0.1549$ and $k_* = 1.26 \times 10^8 \mathrm{Mpc}^{-1}$.

$$\begin{aligned}\Omega_{\rm GW} &\equiv \frac{1}{\rho_{\rm cr}}\frac{\mathrm{d}\rho_{\rm GW}}{\mathrm{d}\ln f} \\ &= 0.29\ \Omega_{\rm r}\left(\frac{106.75}{g_*}\right)^{1/3} \\ &\quad\times\int_0^\infty dv\int_{|1-v|}^{1+v} du\left[\frac{4v^2-(1-u^2+v^2)^2}{4u^2v^2}\right]^2 \\ &\quad\times\left(\frac{u^2+v^2-3}{2uv}\right)^4 F(u,v)P_{\mathcal{R}}(kv)P_{\mathcal{R}}(ku),\end{aligned} \tag{A1}$$

$$\begin{aligned}F(u,v) = &\left(\ln\left|\frac{3-(u+v)^2}{3-(u-v)^2}\right| - \frac{4uv}{u^2+v^2-3}\right)^2 \\ &+\pi^2\Theta\left(u+v-\sqrt{3}\right),\end{aligned} \tag{A2}$$

g_* is the total degree of freedom for massless particles when the mode k enters horizon ($k = aH$) [54, 55], Θ is the Heaviside step function, and the frequency f is related to the wavenumber k via [35],

$$f = 1.546\times10^{-15}\left(\frac{k}{\mathrm{Mpc}^{-1}}\right)\mathrm{Hz} \tag{A3}$$

In addition to emitting SIGW, sufficiently large $P_{\mathcal{R}}$ will also generate overdense regions that can gravitationally collapse into PBHs with mass [7, 35, 56–58],

$$m = 2.43\times10^{-4}\left(\frac{\gamma}{0.2}\right)\left(\frac{g_*}{106.75}\right)^{-1/6}\left(\frac{k}{10^8\mathrm{Mpc}^{-1}}\right)^{-2} m_\odot, \tag{A4}$$

here γ is the collapse efficiency, for which we adopt a typical value of $\gamma = 0.2$ following [35, 56, 58]. The corresponding distribution of PBH abundance is given by [44, 58–60],

$$\begin{aligned}\psi &\equiv \frac{\mathrm{d}f_{\rm bh}}{\mathrm{d}\ln m} \\ &= 0.28\left(\frac{\beta}{10^{-8}}\right)\left(\frac{\gamma}{0.2}\right)^{3/2}\left(\frac{g_*}{106.75}\right)^{-1/4}\left(\frac{m}{m_\odot}\right)^{-1/2},\end{aligned} \tag{A5}$$

where

$$\beta(m) \simeq \sqrt{\frac{2\bar{\sigma}^2}{\pi\delta_{\rm c}^2}}\exp\left(-\frac{\delta_{\rm c}^2}{2\bar{\sigma}^2}\right), \tag{A6}$$

$$\bar{\sigma}^2(m) = \frac{16}{81}\int\mathrm{d}\ln k'\left(\frac{k'}{k}\right)^4 P_{\mathcal{R}}(k')W^2\left(\frac{k'}{k}\right), \tag{A7}$$

here $\delta_{\rm c}$ is the threshold for gravitational collapse, for which we adopt 0.45 following [7, 44, 61, 62]. $W(x)$ is a window function, which we use $\exp(-x^2/2)$ [7, 35, 58].

In Fig. 3 we show the comparison of SIGW posterior and the PTA data, Fig. 4 illustrates the ψ fitting accuracy of Eq. (2).

[1] Y. B. Zel'dovich and I. D. Novikov, Soviet Astron. AJ (Engl. Transl.), **10**, 602 (1967).
[2] B. J. Carr and S. W. Hawking, Mon. Not. Roy. Astron. Soc. **168**, 399 (1974).
[3] B. P. Abbott et al. (LIGO Scientific, Virgo), Phys. Rev. X **9**, 031040 (2019), 1811.12907.
[4] S. Bird, I. Cholis, J. B. Muñoz, Y. Ali-Haïmoud, M. Kamionkowski, E. D. Kovetz, A. Raccanelli, and A. G. Riess, Phys. Rev. Lett. **116**, 201301 (2016), 1603.00464.
[5] B. Carr and F. Kuhnel, SciPost Phys. Lect. Notes **48**, 1 (2022), 2110.02821.
[6] G. Domènech, Universe **7**, 398 (2021), 2109.01398.
[7] J. Cang, Y.-Z. Ma, and Y. Gao, Astrophys. J. **949**, 64 (2023), 2210.03476.
[8] V. Domcke, C. Garcia-Cely, and N. L. Rodd, Phys. Rev. Lett. **129**, 041101 (2022), 2202.00695.
[9] G. Agazie et al. (NANOGrav), Astrophys. J. Lett. **951**, L8 (2023), 2306.16213.
[10] H. Xu et al., Res. Astron. Astrophys. **23**, 075024 (2023), 2306.16216.
[11] D. J. Reardon et al., Astrophys. J. Lett. **951**, L6 (2023), 2306.16215.
[12] J. Antoniadis et al. (EPTA) (2023), 2306.16226.
[13] J. Antoniadis et al. (EPTA) (2023), 2306.16214.
[14] Z. Arzoumanian et al. (NANOGrav), Astrophys. J. Lett. **905**, L34 (2020), 2009.04496.
[15] S. Chen et al., Mon. Not. Roy. Astron. Soc. **508**, 4970 (2021), 2110.13184.
[16] B. Goncharov et al., Astrophys. J. Lett. **917**, L19 (2021), 2107.12112.
[17] J. Antoniadis et al., Mon. Not. Roy. Astron. Soc. **510**, 4873 (2022), 2201.03980.
[18] G. Franciolini, A. Iovino, Junior., V. Vaskonen, and H. Veermae (2023), 2306.17149.
[19] A. Afzal et al. (NANOGrav), Astrophys. J. Lett. **951**, L11 (2023), 2306.16219.
[20] H. Middleton, A. Sesana, S. Chen, A. Vecchio, W. Del Pozzo, and P. A. Rosado, Mon. Not. Roy. Astron. Soc. **502**, L99 (2021), 2011.01246.
[21] L. Bian, R.-G. Cai, J. Liu, X.-Y. Yang, and R. Zhou, Phys. Rev. D **103**, L081301 (2021), 2009.13893.
[22] Z. Arzoumanian et al. (NANOGrav), Phys. Rev. Lett. **127**, 251302 (2021), 2104.13930.
[23] X. Xue et al., Phys. Rev. Lett. **127**, 251303 (2021), 2110.03096.
[24] D. Wang (2022), 2201.09295.
[25] D. Wang (2022), 2203.10959.
[26] R. Z. Ferreira, A. Notari, O. Pujolas, and F. Rompineve, JCAP **02**, 001 (2023), 2204.04228.
[27] K. Inomata, M. Kawasaki, K. Mukaida, and T. T. Yanagida (2023), 2309.11398.
[28] P. Hunt and S. Sarkar, JCAP **12**, 052 (2015), 1510.03338.
[29] N. Planck Collaboration, Aghanim et al. (Planck), Astron. Astrophys. **641**, A6 (2020), [Erratum: Astron.Astrophys. 652, C4 (2021)], 1807.06209.
[30] M. Punturo et al., Class. Quant. Grav. **27**, 194002 (2010).
[31] S. Kawamura et al., PTEP **2021**, 05A105 (2021), 2006.13545.
[32] K. Yagi and N. Seto, Phys. Rev. D **83**, 044011 (2011), [Erratum: Phys.Rev.D 95, 109901 (2017)], 1101.3940.
[33] K. Inomata and T. Nakama, Phys. Rev. D **99**, 043511 (2019), 1812.00674.
[34] S. Pi and M. Sasaki, JCAP **09**, 037 (2020), 2005.12306.
[35] P. Chen, S. Koh, and G. Tumurtushaa, arXiv e-prints arXiv:2107.08638 (2021), 2107.08638.
[36] M. Raidal, C. Spethmann, V. Vaskonen, and H. Veermäe, JCAP **02**, 018 (2019), 1812.01930.
[37] G. Hütsi, M. Raidal, V. Vaskonen, and H. Veermäe, JCAP **03**, 068 (2021), 2012.02786.
[38] A. Hall, A. D. Gow, and C. T. Byrnes, Phys. Rev. D **102**, 123524 (2020), 2008.13704.
[39] P. F. Depta, K. Schmidt-Hoberg, P. Schwaller, and C. Tasillo (2023), 2306.17836.
[40] X.-J. Zhu, E. Howell, T. Regimbau, D. Blair, and Z.-H. Zhu, Astrophys. J. **739**, 86 (2011), 1104.3565.
[41] G. Franciolini, D. Racco, and F. Rompineve (2023), 2306.17136.
[42] Y.-Y. Li, C. Zhang, Z. Wang, M.-Y. Cui, Y.-L. S. Tsai, Q. Yuan, and Y.-Z. Fan (2023), 2306.17124.
[43] P. F. de Salas and S. Pastor, JCAP **07**, 051 (2016), 1606.06986.
[44] B. Carr and F. Kuhnel, Ann. Rev. Nucl. Part. Sci. **70**, 355 (2020), 2006.02838.
[45] F. Feroz, M. P. Hobson, and M. Bridges, Mon. Not. Roy. Astron. Soc. **398**, 1601 (2009), 0809.3437.
[46] A. Lewis (2019), 1910.13970.
[47] E. Thrane and J. D. Romano, Phys. Rev. D **88**, 124032 (2013), 1310.5300.
[48] J. García-Bellido, S. Jaraba, and S. Kuroyanagi, Phys. Dark Univ. **36**, 101009 (2022), 2109.11376.
[49] D. Reitze et al., Bull. Am. Astron. Soc. **51**, 035 (2019), 1907.04833.
[50] P. Auclair et al. (LISA Cosmology Working Group), Living Rev. Rel. **26**, 5 (2023), 2204.05434.
[51] V. Vaskonen and H. Veermäe, Phys. Rev. D **101**, 043015 (2020), 1908.09752.
[52] K. Ando, K. Inomata, and M. Kawasaki, Phys. Rev. D **97**, 103528 (2018), 1802.06393.
[53] K. Kohri and T. Terada, Phys. Rev. D **97**, 123532 (2018), 1804.08577.
[54] E. W. Kolb and M. S. Turner, *The early universe*, vol. 69 (CRC press, 1990).
[55] B. Wallisch, Ph.D. thesis, Cambridge U. (2018), 1810.02800.
[56] B. J. Carr, K. Kohri, Y. Sendouda, and J. Yokoyama, Phys. Rev. D **81**, 104019 (2010), 0912.5297.
[57] T. Nakama, J. Silk, and M. Kamionkowski, Phys. Rev. D **95**, 043511 (2017), 1612.06264.
[58] O. Özsoy, S. Parameswaran, G. Tasinato, and I. Zavala, JCAP **07**, 005 (2018), 1803.07626.
[59] S. Young, C. T. Byrnes, and M. Sasaki, JCAP **07**, 045 (2014), 1405.7023.
[60] B. J. Carr, Astrophys. J. **201**, 1 (1975).
[61] I. Musco and J. C. Miller, Class. Quant. Grav. **30**, 145009 (2013), 1201.2379.
[62] T. Harada, C.-M. Yoo, and K. Kohri, Phys. Rev. D **88**, 084051 (2013), 1309.4201.